Highlights

Multi-objective optimization microchannel heat sink with embedded module with ribs and pin-fins

Xuebin LI, Chunquan LI, Hongyan HUANG, Yuanhao ZHENG

- Microchannel cooling in a Low-Temperature Co-fired Ceramic substrate;

- A comparison with the performance of similar designs;

- Numerical study of three parameters of this microchannel heat sink.

Multi-objective optimization microchannel heat sink with embedded module with ribs and pin-fins

Xuebin LI[a],[**], Chunquan LI[a],[**], Hongyan HUANG[a],[*], Yuanhao ZHENG[a]

[a]*Guilin University Of Electronic Technology, No.1 Jinji Road, Qixing District, Guilin, 541004, the Guangxi Zhuang Autonomous Region, China*

Abstract

A new microchannel heat sink with embedded modules with ribs and pin-fins is proposed as an effective solution to realize microchannel heat dissipation within low-temperature co-fired ceramic substrates.

Keywords: Microchannel heat sink, Embedded modules, LTCC, Rib, Pin-fin

1. Introduction

<mark>当前现状</mark>

随着第五代移动通信等技术的发展 [1]，推动了射频技术向高速、小型化和多功能方向的快速发展，电子芯片的热通量也在增加。

芯片产生的高温和芯片附近较大的温度梯度会降低集成电路的功耗。

2. Mathematical modeling of the microchannel heat sink

Fig. 1 shows the schematic design of MCHS-SR and the proposed MCHS-RPFEM.

Embedded module with ribs and pin-fins embedded in microchannel heat sink below chip. Table 1 shows the geometric parameters of the embedded module. To investigate the effect of ribs and pin-fins on fluid flow and heat transfer on the embedded module in MCHS-RPFEM, three parameters were selected to be varied. These three parameters are relative rib height (α), relative pin-fin height (β), and relative number of auxiliary channels (γ).

---

[*]Corresponding author
[**]These authors contributed to the work equllly and should be regarded as co-first authors.

Email address: `hhy7844@guet.edu.cn` (Hongyan HUANG)
[1]This is the specimen author footnote.

3. Numerical method

In this study, the following assumptions were made to simplify the numerical model:

1. Newtonian fluid flow and steady laminar flow are used, and the fluid follows the Hagen-Poiseuille equation.
2. The walls of the channel are rigid.
3. Neglecting the effects of interaction forces, viscous heat, surface tension, and radiative heat transfer.

3.1. Governing equations and boundary conditions

The governing equations are as follow:

Continuity equation:

$$\nabla \cdot \left(\rho_f \vec{u} \right) = 0 \tag{1}$$

Momentum equation:

$$\vec{u} \cdot \nabla \left(\rho_f \vec{u} \right) = -\nabla p + \nabla \cdot \left(\mu_f \nabla \vec{u} \right) \tag{2}$$

Energy equation for the fluid domain:

$$\vec{u} \cdot \nabla \left(\rho_f C_f T_f \right) = \nabla \cdot \left(k_f \nabla T_f \right) \tag{3}$$

Energy conservation equation for the solid domain:

$$\nabla \left(k_s \nabla T_s \right) = 0 \tag{4}$$

Nomenclature

A	area on the chip's upper surface (m^2)
H_{pf}	height of the pin-fin (μm)
H_{rib}	height of the rib (μm)
L_{rib}	length of the rib (μm)
N_{mc}	number of main channels
N_{oc}	number of auxiliary channels
Re	Reynolds number
S_{pf}	Side length of the pin-fin (μm)
W_{rib}	width of the rib (μm)
d_{rib}	distance between the rib (μm)

Greek symbols

α	Relative rib height
β	Relative pin-fin height
γ	Relative number of auxiliary channels
Λ	molecule Knudsen number of water (m)
μ_f	dynamic viscosity of fluid ($kg/(m \cdot s)$)
ρ_f	density of fluid (kg/m^3)
θ	MATD (Mean Absolute Temperature Deviation) (K)

Subscripts

ave	average value
c	chip
ch	channel
env	environmental
f	fluid
in	inlet
max	maximum value
mc	main channels
oc	auxiliary channels
pf	pin-fin
rib	rib
s	solid
tot	total value

Abbreviations

LED	light-emitting diod
LTCC	Low temperature cofired ceramic
MATD	mean absolute temperature deviation
MCHS	microchannel heat sink
MCHS-SR	straight rectangular microchannel
MCHS-REM	microchannels with rib embedded module
MCHS-PFEM	microchannels with pin-fin embedded module
MCHS-RPFEM	microchannel heat sink with embedded module with rib and pin-fin

Table 1: MCHS-RPFEM geometric parameter table

Geometrical parameters	W_{rib}	H_{rib}	d_{rib}	S_{pf}	H_{pf}	H_{ch}
Value, μm	400	1000	1600	300	1000	1000

The density (ρ_f), specific heat (C_f), thermal conductivity (k_f), and viscosity (μ_f) of deionized water are correlated with the temperature as shown below:

where T is the temperature ($^\circ C$)

3.2. Data reduction

The performance of the four microchannel heat sinks was evaluated by their thermal resistance, Mean Absolute Temperature Deviation (MATD), and pressure drop. Thermal resistance is defined as follows [2]:

$$R_{th} = \frac{T_{c.max} - T_{in.max}}{Q_{tot}} \qquad (9)$$

Q_{tot} is the chip's total heat produced, represented as:

$$Q_{tot} = S V_c \qquad (10)$$

3.3. Grid independence

4. Results and discussion

4.1. Numerical validations

To verify the accuracy of this simulation scheme, the numerical results are compared with the experimental data of several experiments [3–5], as shown in Fig. 2.

4.2. Effect of geometric prameters on hydrothermal performance

In order to explore the influence of the geometric

4.2.1. The effect of relative rib height
4.2.2. Performance analysis

5. Conclusion

To investigate the effect of

Declaration of Competing Interest

The authors declare that they have no known competing financial interests or personal relationships that could have appeared to influence the work reported in this paper.
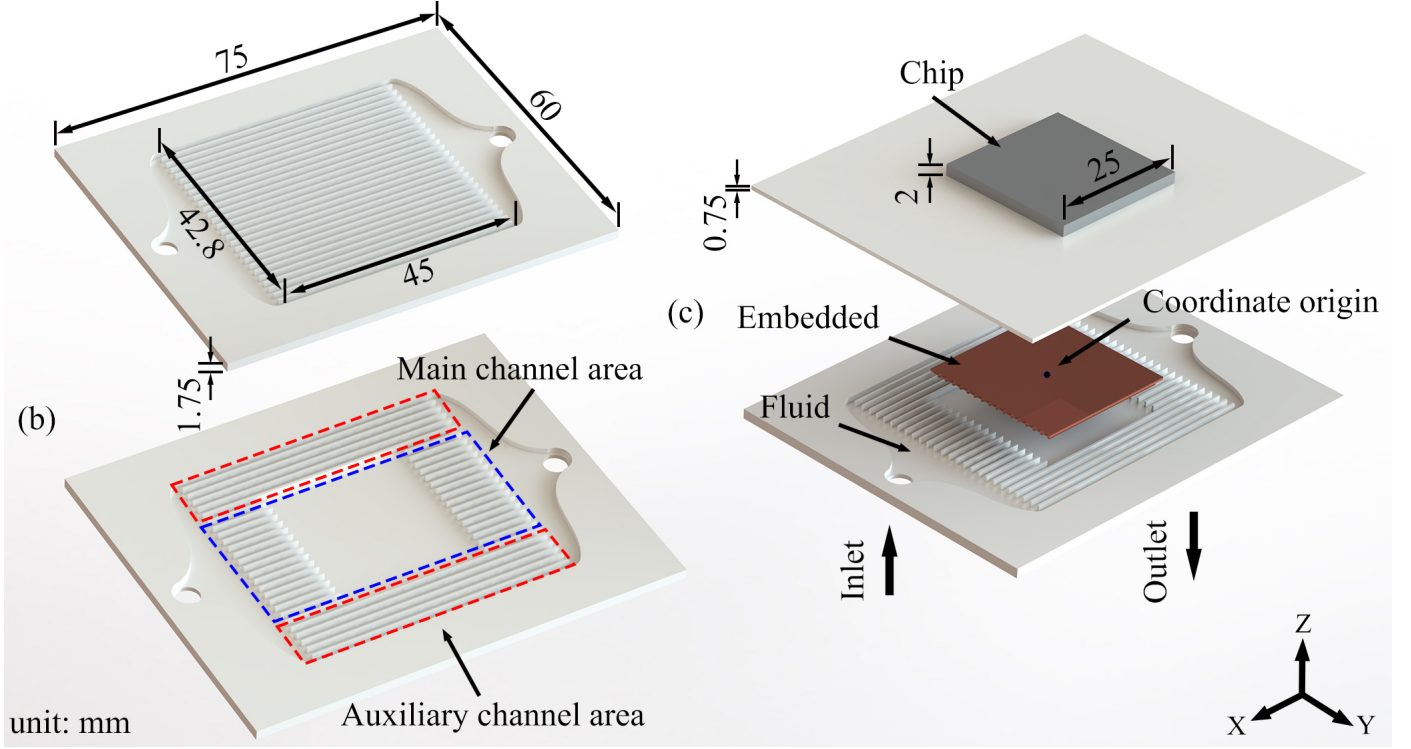
Fig. 1: (a) Straight rectangular microchannel (MCHS-SR), (b) microchannel heat sink with embedded modules with ribs and pin-fins (MCHS-RPFEM), (c) schematic diagram of the structure of MCHS-RPFEM.

$$\rho_f(T) = 999.9 + 9.561 \times 10^{-2}T - 1.013 \times 10^{-2}T^2 + 8.459 \times 10^{-5}T^3 - 3.496 \times 10^{-7}T^4 \tag{5}$$

$$C_f(T) = 4217 - 3.452T + 1.155 \times 10^{-1}T^2 - 1.862 \times 10^{-3}T^3 + 1.538 \times 10^{-5}T^4 - 4.850 \times 10^{-8}T^5 \tag{6}$$

$$k_f(T) = 5.698 \times 10^{-1} + 1.772 \times 10^{-3}T - 4.870 \times 10^{-6}T^2 - 2.915 \times 10^{-8}T^3 + 1.094 \times 10^{-10}T^4 \tag{7}$$

$$\mu_f(T) = 1.750 \times 10^{-3} - 5.558 \times 10^{-5}T + 1.172 \times 10^{-6}T^2 - 1.579 \times 10^{-8}T^3 + 1.169 \times 10^{-10}T^4$$
$$- 3.535 \times 10^{-13}T^5 \tag{8}$$

Table 2: Comparison with other solutions

Reference	Cooling methods	Heating area (mm^2)	Heat power (W)	Flow rate (ml/min)	Inlet pressure (KPa)	Maximum temperature ($^\circ C$)
Zhang et al. [6]	parallel cooling microchannels	22×22	75	58.1	330	99.52
					0.096*	55.7*
Yin et al. [7]	LTCC with embedded metal pillar arrays	21×21	20	18.85	7.12	74.85
					0.021*	57.35*
Liu et al. [8]	LTCC with via holes and liquid metal	10×10	30**	70	-	83.85
					0.138*	95.74*
Yu et al. [9]	LTCC with dual-layer spirals microchannels	2×10	23**	45	370.7	84.85
					0.071*	55.54*

* The heat sink is MCHS-RPFEM and the coolant is deionized water.
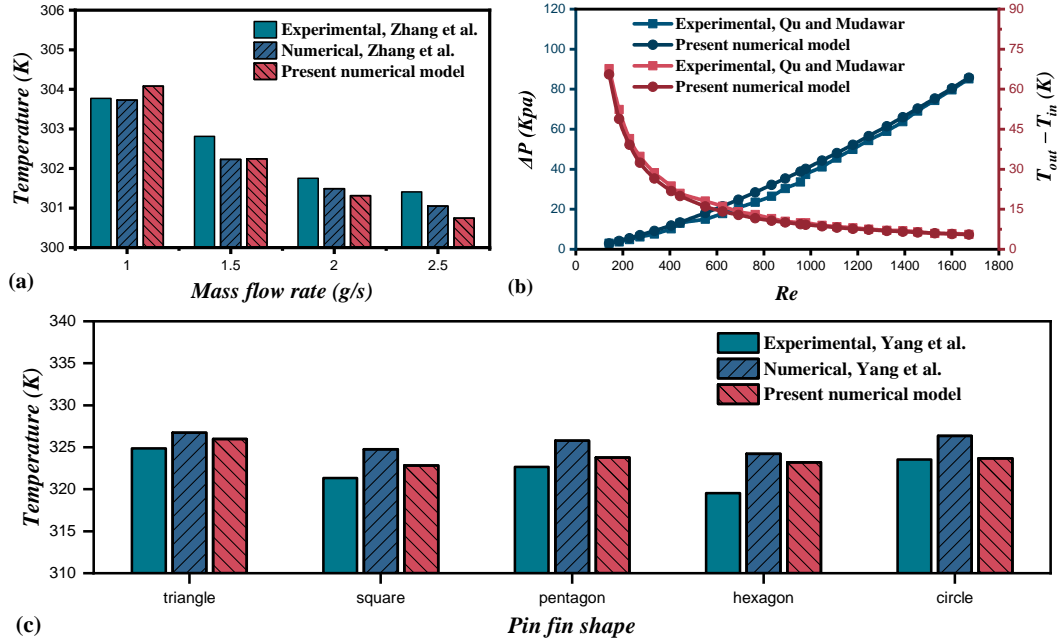** Heat flux(W/cm^2)

Fig. 2: Numerical validations. (a)Zhang et al. [3] of the microchannel heat sink at different mass flow rates for the variation of the bottom surface temperature of the microchannel heat sink. (b)Variation of inlet and outlet temperature difference and pressure drop in microchannels of Qu and Mudawar [4] at different Reynolds numbers. (c)Yang et al. [5] of the pin-fin heat sink with the highest temperature on the bottom surface of the pin-fin heat sink for different pin-fin shapes.

Formatting of funding sources

References

[1] J. H. Lau, Recent Advances and Trends in Advanced Packaging, IEEE Transactions on Components, Packaging and Manufacturing Technology 12 (2) (2022) 228–252. doi:10.1109/TCPMT.2022.3144461.

[2] D. Ansari, J. H. Jeong, A silicon-diamond microchannel heat sink for die-level hotspot thermal management, Applied Thermal Engineering 194 (2021) 117131. doi:10.1016/j.applthermaleng.2021.117131.

[3] F. Zhang, B. Wu, B. Du, Heat transfer optimization based on finned microchannel heat sink, International Journal of Thermal Sciences 172 (2022) 107357. doi:10.1016/j.ijthermalsci.2021.107357.

[4] W. Qu, I. Mudawar, Experimental and numerical study of pressure drop and heat transfer in a single-phase micro-channel heat sink, International Journal of Heat and Mass Transfer 45 (12) (2002) 2549–2565. doi:10.1016/S0017-9310(01)00337-4.

[5] D. Yang, Y. Wang, G. Ding, Z. Jin, J. Zhao, G. Wang, Numerical and experimental analysis of cooling performance of single-phase array microchannel heat sinks with different pin-fin configurations, Applied Thermal Engineering 112 (2017) 1547–1556. doi:10.1016/j.applthermaleng.2016.08.211.

[6] L.-Y. Zhang, Y.-F. Zhang, J.-Q. Chen, S.-L. Bai, Fluid flow and heat transfer characteristics of liquid cooling microchannels in LTCC multilayered packaging substrate, International Journal of Heat and Mass Transfer 84 (2015) 339–345. doi:10.1016/j.ijheatmasstransfer.2014.12.079.

[7] P. Yin, Y. Li, P. Zhang, G. Xiao, H. Yuan, On-chip heat dissipation design for high-power SiP modules with LTCC substrates, in: 2019 20th International Conference on Electronic Packaging Technology(ICEPT), 2019, pp. 1–4. doi:10.1109/ICEPT47577.2019.245096.

[8] N. Liu, Y. Jin, M. Miao, X. Cui, Optimization of heat transfer of microchannels in LTCC substrate with via holes and liquid metal, in: 2016 17th International Conference on Electronic Packaging Technology (ICEPT), 2016, pp. 1135–1139. doi:10.1109/ICEPT.2016.7583325.

[9] H. YU, B. HAN, M. MIAO, X. CUI, K. ZHAO, Design and Analysis of Microchannel for the Thermal Management of Multi-stacked LTCC Laminates, in: 2018 19th International Conference on Electronic Packaging Technology (ICEPT), 2018, pp. 872–875. doi:10.1109/ICEPT.2018.8480810.